Desalination and Water Treatment
www.deswater.com

doi: 10.5004/dwt.2017.21496

92 (2017) 172–180
October

Formation of predominant interstitial N–TiO_2 using physical preparation under microwave irradiation for Reactive Red 4 dye removal

M.S. Azami[a,b], W.I. Nawawi [a,c,*], D.S.M. Shukri[a]

[a]*Photocatalysis Laboratory, CBERG, Faculty of Applied Sciences, Universiti Teknologi MARA, 02600 Arau, Perlis, Malaysia, Tel. +60 49882305; Fax: +6049882026; email: wi_nawawi@perlis.uitm.edu.my (W.I. Nawawi), Tel. +60 167603950; email: saifulddinazami@gmail.com (M.S. Azami), Tel. +60137143940; email: dyia839@perlis.uitm.edu.my (D.S.M. Shukri)*
[b]*Faculty of Applied Sciences, Universiti Teknologi MARA, 40450 Shah Alam, Selangor, Malaysia*
[c]*Department of Chemistry, University of York, Heslington, York, YO10 5DD, UK*

Received 25 January 2017; Accepted 26 September 2017

ABSTRACT

Interstitial nitrogen titanium dioxide (N–TiO_2) has been synthesized from solid-state microwave irradiation of commercial TiO_2 (P25) and urea, which is in contrast to other solid-state methods that give substitutional N–TiO_2. N–TiO_2 was characterized by powder X-ray diffraction (XRD), N_2-adsorption surface area measurement, Fourier transformed infra-red (FTIR), X-ray photoelectron spectroscopy (XPS) and UV-Vis diffuse reflectance spectroscopy (UV-Vis DRS). FTIR, XPS and UV-Vis DRS indicate that interstitial doping of N has occurred in the TiO_2 lattice. Ti–O–N detected by FTIR at 1,449 cm^{-1} contributed to the N–O bond. There is no C=O bond in N–TiO_2 showing that urea was completely decomposed in modified TiO_2. This N–O bond is also proved by XPS on deconvolution peaks detected at 404.8 and 531.5 eV in N 1s and O 1s, respectively. UV-Vis DRS analysis revealed the formation of N 2p state ca. 0.12 eV above valence band in N–TiO_2 and it is almost similar to characteristic of substitutional N–TiO_2. Thus, the combination of substitutional and interstitial called interstitial N 2p is suggested in our prepared N–TiO_2 sample. The photocatalytic activities of N–TiO_2 and pristine TiO_2 were compared for the photodegradation of the dye reactive red 4 (RR4) under visible light irradiation from an LED source. Complete bleaching occurred within 60 min using N–TiO_2 whereas no photocatalytic degradation was observed using pristine TiO_2.

Keywords: Interstitial N 2p; Nitrogen doping; Photocatalysis; Microwave; Reactive red 4 dye

1. Introduction

There have been numerous attempts to extend the photocatalytic activity of TiO_2 into the visible light region of the solar spectrum for the photodegradation of organic pollutants. These include the modification of TiO_2 via nitrogen doping discovered by Sato [1] who reported a visible light active photocatalyst prepared by reaction between NO_x and TiO_2 using tetrafluoroammoniumoxyhydride (NF_4OH) as the NO_x source. Asahi et al. [2] also showed N-doping of TiO_2 prepared by sputtering TiO_2 in an N_2/Ar gas mixture resulting in a material showing photocatalytic activity under visible light irradiation in contrast to pristine TiO_2. Furthermore, N doping of TiO_2 was proposed to occur substitutionally introducing N 2p states that mix with the predominantly O 2p valence band (VB) effectively narrowing the bandgap. In contrast, Valentin et al. [3] performed density functional theory (DFT) calculations describing substitutional doping of rutile and anatase phases showing that N-doping leads to localized N 2p states within the bandgap. For anatase, these states are ca. 0.14 eV above the VB thus decreasing the threshold for optical absorption, whereas for rutile N-doping results in localized states but also a narrowing of the O 2p VB with the net effect of increasing the optical threshold [3]. While an interstitial N–TiO_2 formed by forming π character generated by N–O bond where an electronic state

* Corresponding author.

lied at 0.73 eV above of the VB [3]. In a related report, substitutional and interstitial N-doping were considered for anatase showing that interstitial N-doping also leads to localized states which are higher in energy than substitutional doping due to O–N π-antibonding interactions giving a lower threshold for optical absorption [4]. Experimentally, X-ray photoelectron spectroscopy (XPS) can potentially differentiate between interstitial and substitutional N–TiO_2 based on binding energy of deconvolution peaks in N 1s spectra, where below 399 eV is attributed to N-substitution with O–Ti–N bonding while interstitial N–TiO_2 can be interpreted as Ti–O–N or Ti–N–O bonding which can be observed above 399 eV [5].

N-doping is dependent on the synthetic methods and post-synthetic treatments, including from Ti and N molecular precursors and modification of solid TiO_2 single crystals or powders. Preparation of interstitial N–TiO_2 generally involves a wet process of urea such as hydrothermal, solvothermal or sol-gel reactions [6–10]. For example, Peng et al. [9] prepared a yellow powder of N–TiO_2 from P25 and urea in ethylene glycol solvothermally producing interstitial N shows the binding energies of N 1s at 399.9 eV while the N–TiO_2 annealed under NH_3 producing substitutional N shows the binding energies of N 1s at 396.5 eV. The interstitial N shows higher photodegradation under visible light compared with substitutional N. The use of a co-hydrothermal method from TiO_2-P25 and urea in 10 M sodium hydroxide (NaOH) by Hu et al. [10] showed the binding energy of N at 399.9 eV producing interstitial diffusion of nitrogen. Both of these studies producing hyponitrite $(N_2O_2)^{2-}$ in their nitrogen doped as can see in their binding energy of O 1s at 531.5 and 531.1 eV, respectively. The formation of hyponitrite was due to the N interstitially doping into the TiO_2 lattice [9,10].

In comparison, substitutional N–TiO_2 is usually prepared by urea under solid-state methods where TiO_2 powder is physically mixed with a nitrogen precursor. Rengifo et al. [11] found that heating TiO_2 and urea at 400°C gave substitutional N–TiO_2 used to photodegrade *Escherichia coli* under visible light irradiation while Kang et al. [12] also reported substitutional N–TiO_2 prepared by physical process reduced of its bandgap energy. Previously, we also showed substitutional N-doping from reaction between TiO_2 and urea in a semi-closed reactor system at 350°C, in which showed good photodegradation of reactive red 4 (RR4), methyl blue and phenol under visible light irradiation [13]. Most of this N-doped preparation was prepared under furnace as their heating media.

With respect to microwave synthesis of N–TiO_2, a sol-gel prepared from titanium ethoxide and urea was reported by Wu et al. [14] giving almost exclusively substitutional N-doping. Kadam et al. [15] reported that N–TiO_2 nanostructures synthesized by simple microwave-assisted method, between titanium tetraisopropoxide and ammonium hydroxide gave substituted N-doping.

Hence, from the best of our knowledge there is no study focused on the modification of N–TiO_2 using physical preparation under microwave condition which may result either substitutional or interstitial. This preparation will allow the development of more environmental friendly process to produce N–TiO_2 by utilizing urea as N source and more cost-effective process by using commercially available photocatalyst.

Cibacron Brilliant Red dye or typically known as Reactive Red 4 dye is one of the anionic dyes, which is negatively charged, where it is attracted towards positive surface. This dye can be categorized as monoazo dye with one azo (N=N) bond in its structure. Some researchers have documented that some azo dyes are toxic and even mutagenic to living things especially for aquatic life [16]. This is because azo dyes contain toxic aromatic amines. This dye was applied in industry such as printing and dyeing cellulose fibres such as cotton and rayon. Based on the previous study, RR4 is not commonly been used as a model of pollution in research of photocatalysis. Basically, Reactive Red 120 (RR120) and Reactive Red 198 (RR198) are the dyes that are widely used in research whether focusing in photocatalytic degradation, intermediate and adsorption study [17,18].

In this paper, an N–TiO_2 was prepared from reaction between TiO_2-P25 and urea using microwave solid-state synthesis. In contrast to other solid-state reactions that favor predominately substitutional N–TiO_2, we observe evidence suggestive of predominantly interstitial N-doping of TiO_2 and surface modification. N-doping leads to visible light photocatalytic activity for the photodegradation of RR4 dye.

2. Experimental

2.1. Materials

TiO_2 Degussa P25 powder was used as the starting material in the preparation of N–TiO_2. Urea from Fluka, Switzerland (chemical formula: NH_2CONH_2, molecular weight: 60.06 g mol^{-1}) was used as the N precursor. RR4 dye or commonly known as Cibacron Brilliant Red (colour index number: 18105, chemical formula: $C_{32}H_{23}ClN_8Na_4O_{14}S_4$, molecular weight: 995.23 g mol^{-1}, λ max: 517 nm). Ultra-pure water was used to prepare all solutions in this work. LED lamp was used as a visible light source to activate the photocalatytic activity of TiO_2. A domestic microwave oven model Samsung ME711K, which is the source of microwave, was used as a medium for heating as well as to initiate the process of N interstitial formation in TiO_2. The pressure used for the entire process is under atmospheric pressure.

2.2. Modified N–TiO_2 using physical preparation

Interstitial N–TiO_2 was synthesized by mechanically mixing TiO_2 (7 g, 87.5 mmol) with urea (3 g, 50 mmol) for 5 min using a ball mill to give a white powder. This ratio was selected based on the optimum N–TiO_2 which is a continuation from our previous published paper [19]. The mixed powder was placed into a conical flask in the semi-closed reactor and irradiated by using microwave (2,450 MHz) at 800 W for 30 min. The sample was cooled down to the room temperature and the yellow light powder was denoted as N–TiO_2. The phase transformation of the modified N–TiO_2 was investigated using X-ray diffraction (XRD) analysis (Rigaku, Japan, Miniflex II Desktop X-Ray Diffractometer) with a diffraction angle range $2\theta = 10°–80°$ using Cu Kα radiation ($\lambda = 1.5418$ Å) was used to collect XRD diffractograms. The accelerating voltage and emission current were 40 kV and 30 mA, respectively. N_2-adsorption surface area measurement was used to investigate the surface area of photocatalyst. The bandgap

energy of photocatalyst was determined by using Lambda 35 UV-Vis spectrophotometer, from PerkinElmer, USA, equipped with diffuse reflectance attachment at the wavelength of 280–800 nm. Fourier transformed infra-red (FTIR) spectroscopy analysis was conducted to investigate the functional groups in the photocatalyst recorded in the 4,000 to 600 cm^{-1} region. XPS analysis was applied to determine the binding energies of N in TiO_2 and recorded using Omicron NanoTechnology (ELS5000) system using Al Kα radiation at a base pressure below 5.5×10^{-9} torr.

2.3. Photocatalytic activity and adsorption studies

The photocatalytic performances of the N–TiO_2 and pristine TiO_2 samples were investigated in the degradation of RR4 dye under visible light irradiation. The photodegradation activity was carried out by adding 0.03 g of photocatalyst sample into 25 mL of 30 mg L^{-1} RR4 dye to form suspensions. This suspension was then poured into a glass cell with dimension 50 mm × 10 mm × 80 mm (L × B × H) and irradiated with 20 W LED lamp with 237 W m^{-2} light intensity of visible light source. An aquarium pump model NS 7200 was used as an aeration source for oxygen supply. During each photocatalytic experiment, the decolourization degree of RR4 was determined at specific time interval until complete decolourization was achieved. The absorbance was measured by using HACH DR 1900 spectrophotometer at 517 nm. The experimental setup for adsorption study followed the same procedure as photocatalytic activity study except the sample was applied in the dark condition.

3. Result and discussion

3.1. Characterization study of photocatalyst

XRD patterns for N–TiO_2, pristine TiO_2 and TiN samples were presented in Fig. 1. TiN standard sample was used as control sample for the determination of N substitution TiO_2. All peaks in XRD for N–TiO_2 and pristine TiO_2 were detected as anatase and rutile phases with diffraction of anatase signals detected at 25.28°, 37.91°, 41.37°, 48.12°, 53.96°, 55.25°, 62.97°, 70.55°, 75.28° and 82.95° 2θ while peaks at 27.38°, 36.02°, 41.18° 2θ in XRD spectrum were represented as rutile signal in N–TiO_2 and pristine TiO_2. No phase transformation was observed in N–TiO_2 since the process was prepared under low temperature. Phase transformation in the presence of non-metal doped TiO_2 was observed by Zhang et al. [20] to be occurred only when the heating temperature is at 800°C while Wang et al. [21] reported that phase transformation for TiO_2 heated without N occurred at temperature 600°C onwards.

The peaks present in TiN standard sample were detected at 35.9° and 43.23°. According to Xie et al. [22], peak represented as N substitution incorporated with TiO_2 can be detected at 2θ = 43.23°. The similar behaviour was reported by An et al. [23] observed at 2θ = 43° implying the N substitution with TiO_2 formed by N_2 gas during calcination. Irrespective of the concentration of the substituted nitrogen, there were no indications of the existence of TiN observed in N–TiO_2 XRD spectra in Fig. 1. This might be due to the effect of dopant species and it is probably transferring into the position of interstitial in crystallite structure of TiO_2 which is also reported by others [9–11]. Masaaki et al. [24] interpreted that the substitution of nitrogen can be observed in XRD spectrum when the anatase peaks disappeared producing unknown peaks at certain condition. The XRD spectrum of N–TiO_2 shows that anatase phase remained same as pristine TiO_2 spectrum. The crystalline structure of N–TiO_2 and pristine TiO_2 also showed similarity since the pattern for those peaks is almost identical. Hence, it can be assumed that N–TiO_2 synthesis under physical preparation using microwave irradiation does not affect the crystalline structure of TiO_2.

N_2-adsorption surface area measurement was carried out to investigate the specific surface area of the samples. Surface area values of pristine and N–TiO_2 are listed in Table 1. It was observed that surface area of N–TiO_2 sample shows 14% decreasing in comparison with pristine TiO_2. This phenomenon is due to the sintering effect produced from rapid heating of microwave irradiation that reduces the pore size of N–TiO_2 and eventually reducing the surface area of the sample. This solid-state sintering allowed the N particle to diffuse and bond together with TiO_2. Based on solid-state sintering effect theory shown in Fig. 2, particle bonding of N and TiO_2 was started at contact point, which then grows into necks and reducing pores between the particles of TiO_2 [25].

Fourier transforms infrared (FTIR) spectrums of pristine and N–TiO_2 were studied to determine presence

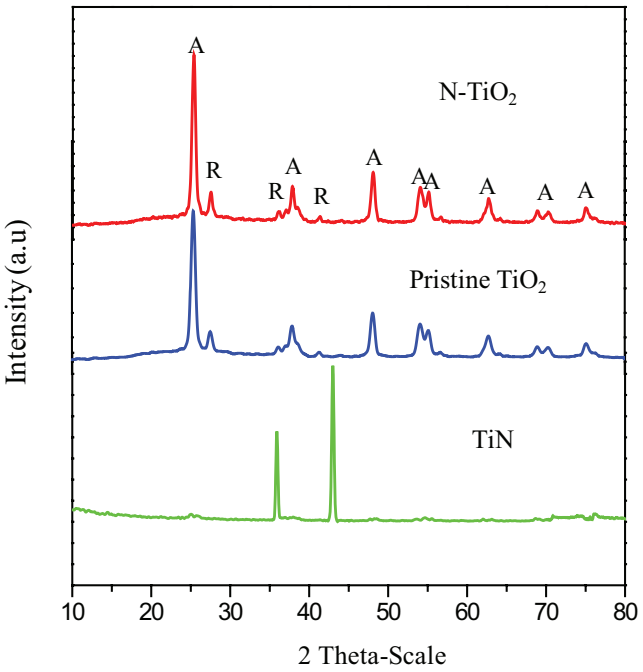

Fig. 1. XRD patterns of N–TiO_2, pristine TiO_2 and TiN.

Table 1
Surface area and bandgap energy of unmodified and modified TiO_2

Samples	S_{BET} (m^2 g^{-1})	E_g (eV)
TiO_2	49.0	3.02
N–TiO_2	44.0	2.9

of N bonding by detecting some N groups in N–TiO_2. FTIR spectra of pristine TiO_2, urea and N–TiO_2 samples are shown in Fig. 3. The characteristic stretching vibration of Ti–O–Ti lattice was found in the signal below 1,000 cm^{-1} of pristine TiO_2 and N–TiO_2. The pristine TiO_2 signal at 3,359 and 1,638 cm^{-1} attributed to the primary O–H stretching of the hydroxyl functional group and bending vibration H–OH group, respectively [26]. The peak at 1,642 cm^{-1} observed in N–TiO_2 was attributed to the bending vibrations of O–H and N–H, and peak at 3,342 cm^{-1} was from stretching vibration of O–H and N–H. Same peaks were observed by Hu et at. [27] who claimed that bending vibration peaks of N–H in amine can be observed at 3,150–3,600 cm^{-1} and 1,600–1,650 cm^{-1}. The small peak appeared at 1,449 cm^{-1} was detected as –N–O_X [28]. No C=O bond was detected in N–TiO_2 representing the element in urea. Thus, FTIR spectrum proved that urea is completely decomposed under microwave producing N–O and N–H bond incorporated with pristine TiO_2 to form N–TiO_2. According to Peng et al. [9], interstitial N–TiO_2 can be interpreted as N–O asymmetric and N–H bonds from TiO_2 surface suggested as hyponitrite or interstitial formation.

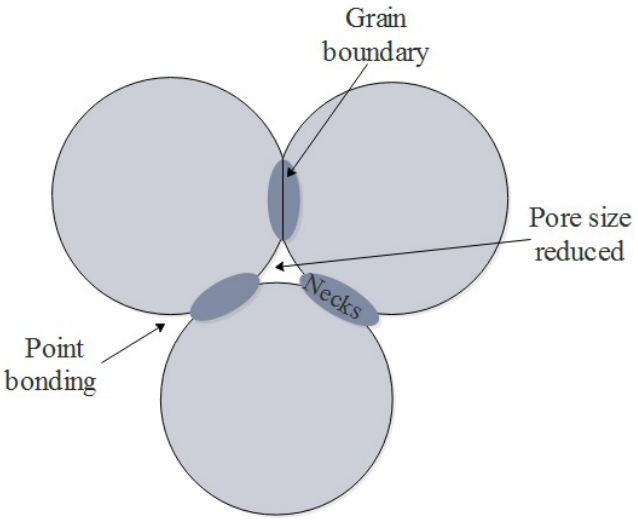

Fig. 2. Solid-state sintering effect of N–TiO_2.

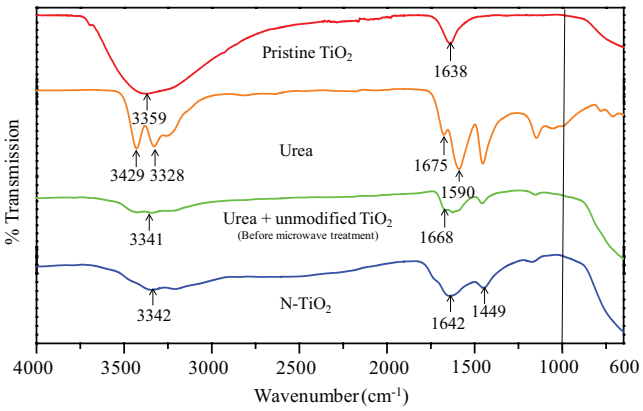

Fig. 3. FTIR spectra of N–TiO_2, urea + unmodified TiO_2, urea and pristine TiO_2.

These N–H and N–O bonds exist in N–TiO_2 sample at 1,642 and 3,342, and 1,449 cm^{-1}, respectively, as well described by Hu et al. [27] and Peng et al. [9]. This explained that the prepared N–TiO_2 sample in this study is a result of the formation of interstitial bonding since N–O and N–H bonds were detected.

XPS analysis was conducted to further confirm the formation of N species whether it is substitutional or interstitial type with O lattice in N–TiO_2. Figs. 4(a)–(c) display the XPS spectra of N 1s, Ti 2p, O 1s for the N–TiO_2 sample, respectively. Fig. 3(a) clearly shows the N 1s spectra with deconvolution peaks detected at 400.3 and 404.8 eV representing interstitial N in the form of N–O bond. However, a few reports on N 1s peak above 400 eV assigned as chemisorbed nitrogen, NH_3 adsorbed on the surface TiO_2 and trapped N_2 gas [29,30]. But, many researchers have agreed and pointed out that the binding energy at 399 eV and above is assigned as interstitial N–O species [10,31–34]. Peak at 404.8 eV of N 1s represented as surface adsorbed nitrogen species which is the nitrogen species bound to various surface oxygen site such as NO, NO_2 or NO_x [35]. Sathish et al. [36] discovered that although the deconvolution N 1s at the peak 400 eV is not proven experimentally but hypothesized that the binding energy of N 1s is higher when the nitrogen atom in a chemical linkage shows more positive formal charge. Consequently, N 1s binding energy at the peak 400.3 eV for N–TiO_2 sample in this study can be attributed to the formation of interstitial N and directly bounded to lattice oxygen. No characteristic of Ti–N peak at 396–397.5 eV was observed which signifies the non-appearances of the substitutional N phase in N–TiO_2 sample as well previously reported in XRD where no substitutional N bond was detected since there is no formation of the TiN phase on N–TiO_2. Thus, the XPS result becomes favourable predominantly toward the formation of interstitial and probably consists minor signal of substitutional N which can be disregarded since the explanation on the formation of interstitial and substitutional is still under disputation.

The XPS spectra of O 1s core level consisting of a major peak at 531.4 eV detected as the formation of hyponitrite $(N_2O_2)^{-2}$ which was caused by the N interstitially doping into the lattice TiO_2 [8,10] is shown in Fig. 4(b). The deconvolution peaks were detected at 530.6 and 532.2 eV and those peaks are assigned as Ti–O bonding of TiO_2 [9,11,37] while Ti 2p spectra for N–TiO_2 shows the deconvolution peaks detected as Ti $2p^{2/3}$ and Ti $2p^{1/2}$ core level at 457.96 and 463.71 eV, respectively in Fig. 4(c). Since TiO_2 bonding is not only with neighbouring Ti atom by Ti–O–Ti linkage but also with the substrate N by Ti–O–N linkages. Therefore, suggesting that Ti 2p peak at 457.96 and 463.71 eV can be assigned to the $Ti^{4+}O_X$ on the N surface. However, Ti 2p spectra at peak 457.96 eV also can be detected as Ti^{3+} defect [38] and it will contribute to the formation of oxygen vacancies in doping nitrogen species [39] where oxygen vacancies can impede toward the recombination of carrier charge and encourage to electron transfer.

Fig. 5(a) shows the UV-Vis diffuse reflectance spectroscopy (UV-Vis DRS) spectra for pristine and N–TiO_2 samples. From Fig. 5(a), it can be observed that the absorption edge of unmodified TiO_2 is around 400 nm while for N–TiO_2 it is around 430 nm. The wavelength range for UV light is from 200 to 400 nm while wavelength for visible light is

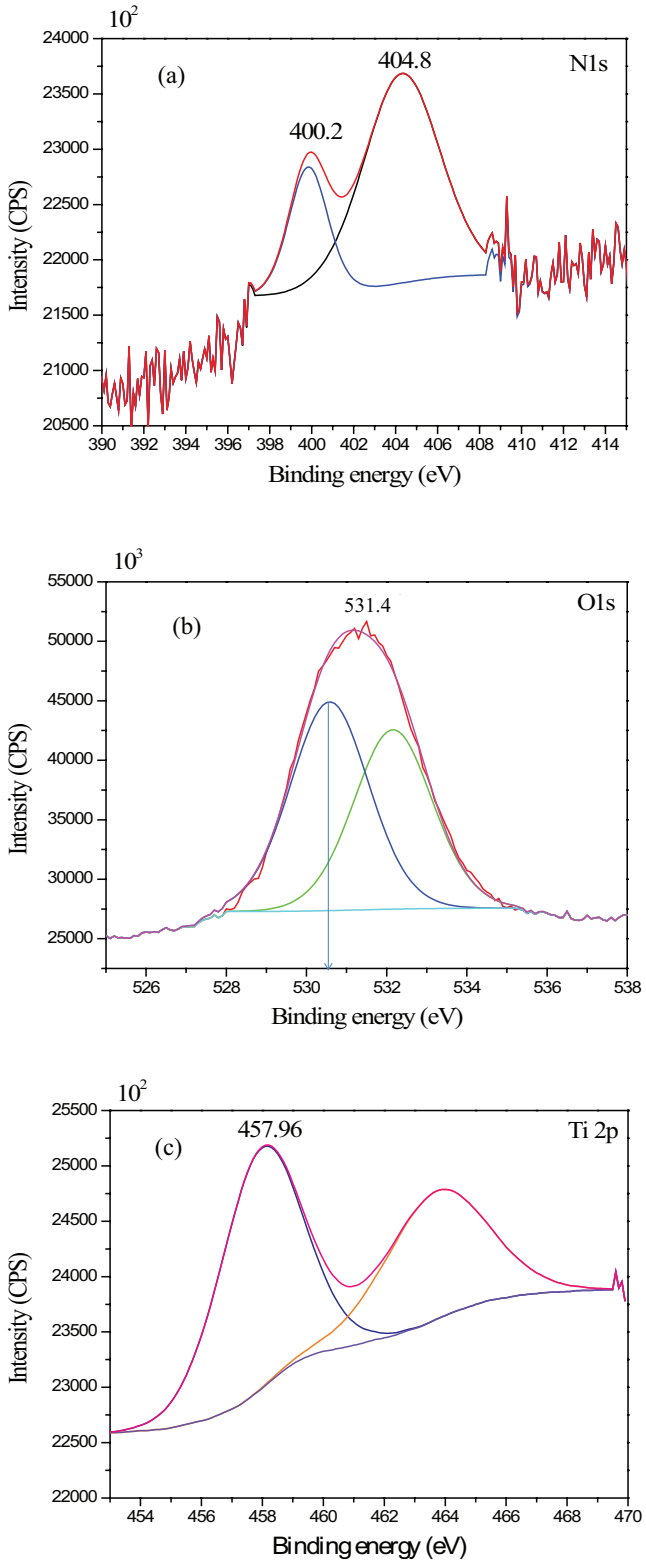

Fig. 4. XPS spectra of N–TiO_2 sample for (a) N 1s, (b) O 1s and (c) Ti 2p.

from 401 to 700 nm [5]. N–TiO_2 sample shows the shift of its absorption towards the visible light region in comparison with pristine TiO_2 absorption edge within the UV region.

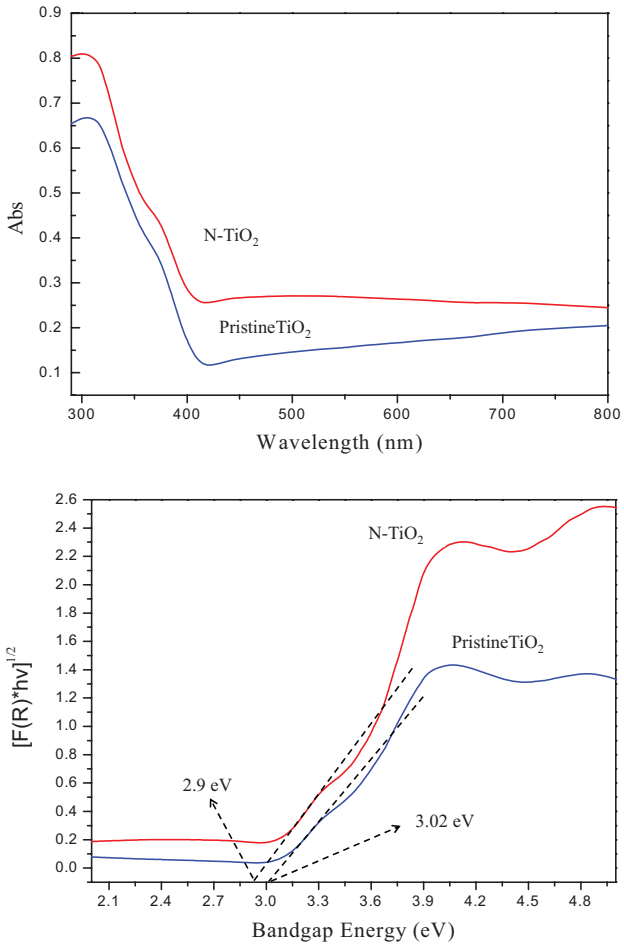

Fig. 5. UV-Vis DRS graph of pristine TiO_2 and N–TiO_2 (a), and (b) Tauc's plot of pristine TiO_2 and N–TiO_2.

This observation shows that N atom in urea was significantly reacted with TiO_2 particles producing oxygen vacancy and defect thus, narrowing bandgap energy of photocatalyst. According to Tauc and Menth [40], the absorption coefficient can be described as a function of incident photon energy stated in Eq. (1).

$$(\alpha h\nu)^2 = A\,(h\nu - E_g) \quad (1)$$

where α is the absorption coefficient (cm^{-1}), A is a constant, $h\nu$ (eV) is the energy of excitation and E_g the bandgap energy. The bandgap energy can be measured by plotting $(\alpha h\nu)^2$ vs. $h\nu$ called Tauc's plot and extrapolation slope on the photon energy axis gives the value of the direct bandgap energy of semiconductors.

Fig. 5(b) shows Tauc's plot of $(\alpha h\nu)^2$ vs. $h\nu$ for pristine TiO_2 and N–TiO_2. Based on extrapolation slope in Fig. 5(b), bandgap energy for pristine TiO_2 was measured and it is around 3.02 eV while the bandgap for N–TiO_2 is around 2.9 eV. It is clearly shown that bandgap energy value for N–TiO_2 is low when compared with pristine TiO_2 and obviously shows that N atom in urea was significantly reacted with TiO_2 particles producing defect structure as previously

explained. This observation is in line with other researchers where Peng et al. [41] reported narrowed bandgap energy of photocatalyst was due to the introducing of the impurity level between the valence and conduction band (CB) of TiO_2. Nawawi and Nawi [42] also reported that the narrowing bandgap is associated with the doping of N in modified photocatalyst.

3.2. Mechanism for interstitial N 2p N–TiO_2

In this study, Ti bonded with O to form TiO_2, which is a type of metal oxide. The combination of these two creates VB and CB with bandgap between them. The larger the bandgap, the less conductive and photoactivity the material will be. Therefore, a decrease in bandgap is preferable in increasing conductivity and photoactivity. In this study, N enters the TiO_2 matrix by means of interstitial forming Ti–O–N. As can be observed in the UV-Vis DRS spectra, bandgap energy for prepared N–TiO_2 is 0.12 eV which is lower compared with pristine TiO_2. It means that an N 2p state is formed at 0.12 eV above VB in prepared N–TiO_2. According to Valentin et al. [4], substitutional N 2p localized is slightly above VB with 0.14 eV which is almost similar to our prepared N–TiO_2. However, XPS reading on our prepared sample indicates the sign of interstitial N formation in N–TiO_2 detected at 400.2 and 404.8 eV in deconvolution peaks of N 1s while FTIR also revealed the interstitial N formation at 1,538 cm^{-1}. From previous studies, XPS peaks above 400 eV indicates interstitial N which p* molecular orbitals that formed from N–O species lied about 0.73 eV above the VB [4,9] where it was not observed in our sample. Since N and O atoms are closely similar to each other based on chemical properties forming either interstitial Ti–O–N or substitutional N–Ti–O. Thus, the combination of substitutional and interstitial called interstitial N 2p is suggested in our prepared N–TiO_2 sample. The similar effect and formation of interstitial N 2p for N–TiO_2 were also reported by Kim et al. [43] and Lin et al. [31] in their preparation using wet chemical method using aqueous ammonia. The schematic diagram of electronic band for substitution, interstitial and interstitial N 2p was depicted in Fig. 6.

3.3. Adsorption and photocatalytic studies

In this study, anionic RR4 dye was used to determine the adsorption capacity in N–TiO_2. Based on Fig. 7, it shows both of pristine and N–TiO_2 are managed to adsorb almost 50% of 30 mg L^{-1} RR4 dye with adsorption of N–TiO_2 shows higher than pristine TiO_2. Higher adsorption rate normally related to high specific surface area which attracted more dye substrates to its surface [42,44]. The degradation of organic pollutants by TiO_2 photocatalyst occurs primarily on or near the surface of the catalyst and thus adsorption is a critical factor in the efficiency of the process. Larger specific surface area means more adsorption sites. Sample with larger specific surface area can pre-adsorb more dye molecules on the surface of sample. However, the surface area results show different where pristine TiO_2 with high surface area shows a slightly lower of its adsorption by 10% compared with N–TiO_2 (Table 1). This is due to the coulombic attraction by the positive charge of pristine TiO_2 and N–TiO_2 proven by measuring these photocatalysts by using zeta potential at ambient condition (pH 5.5). The zeta potential value of unmodified TiO_2 was measured about 0.79 mV while the zeta potential for N–TiO_2 was 15.57 mV and this explained adsorption of RR4 under N–TiO_2 was higher than pristine TiO_2.

Fig. 8 shows the photocatalytic degradation of RR4 dye of pristine and N–TiO_2 irradiated under LED lamp as visible light

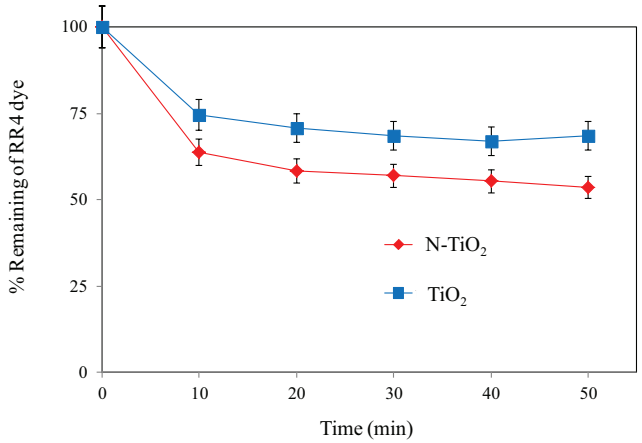

Fig. 7. The adsorption study of pristine and N–TiO_2 under 30 mg L^{-1} RR4 dye.

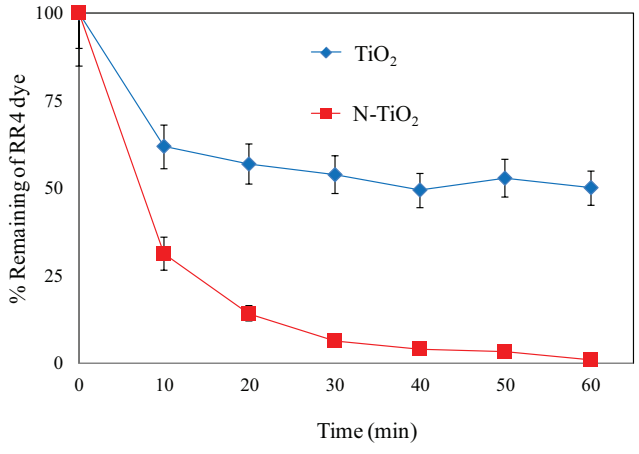

Fig. 8. Photocatalytic degradation of pristine TiO_2 and N–TiO_2 under visible light irradiation.

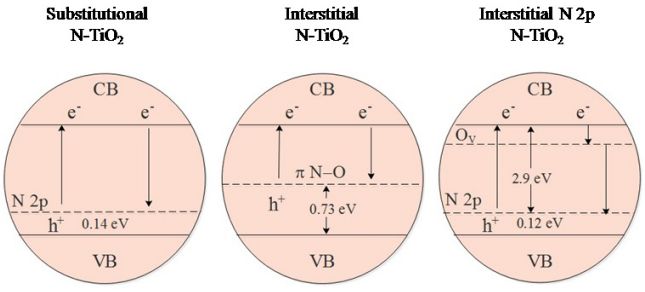

Fig. 6. Electronic band for substitution, interstitial and interstitial N2p.

source. The intensity for LED lamp was measured by solar radiometer model PMA 2100 with visible light intensity was 237 W m^{-2} with no UV radiation detected. It was observed that N–TiO_2 takes only 60 min to complete the decolourization of RR4 while no photocatalytic degradation under pristine TiO_2 was observed. However, RR4 dye decolourized about 40% for 30 min and no decolourization was detected after prolonging the irradiation under pristine TiO_2. The RR4 decolourization under pristine TiO_2 was due to the adsorption of TiO_2 particle since the same trend observed on pristine TiO_2 under both adsorption and photocatalytic studies as can be seen in Figs. 7 and 8, respectively. N–TiO_2 contributed positive result when it was active under visible light irradiation. Hence, the distinction of photocatalytic activity between pristine TiO_2 and N–TiO_2 samples is not persuaded by the specific surface area. In the process of photo-oxidation, pristine TiO_2 photocatalyst is not sufficient to excite electron of the visible light energy from VB to CB as the intrinsic bandgap of pristine TiO_2. Based on the result of XRD, FTIR, XPS and UV-Vis DRS analyses, N atoms were incorporated into the crystalline TiO_2 producing the formation of Ti–O–N structure which suggested the interstitial N 2p. Interstitial N 2p in N–TiO_2 encouraged the localized occupied states forming a mid-bandgap that enhanced photocatalysis under visible light irradiation [31]. Fig. 9 shows the proposed schematic diagram of interstitial N 2p N–TiO_2 in photodegradation of RR4 dye under visible light. VB electrons (e^-) are excited from N 2p level to the CB. e^- in the CB will trap rapidly by molecular of oxygen adsorbed on the particle. The formation of oxygen vacancy (O_V) which was below the CB was formed from the N-doping species. This formation was an indirect correlation with interstitial N 2p, as the concentration of interstitial N 2p increases, O_V will also increases [45]. Hence, the electrons are excited from N 2p level bond to the O_V level then recombine with hole (h^+). The photogenerated holes will react with hydroxide ion, OH^-, or water to oxidize them into hydroxyl radicals (•OH) [46]. The photogenerated electron in CB reacted with O and reduced the trapped O to form superoxide radical anion (O_2•$^-$). The protonation of O_2•$^-$ producing perhydroxyl radical (•OOH). The protonation yield •OOH radical which trapping electron and combine to produce H_2O_2. The surface O_V induced by microwave treatment was trapped the electron and promoted to form more superoxide anion radical (O_2•$^-$) which then interact with adsorbed H_2O to produce more •OH radicals. The •OH radicals react with RR4 and mineralize into CO_2 and H_2O. Thus, it is proven that the formation of interstitial N 2p in TiO_2 reduced the bandgap energy of N–TiO_2 and producing O_V promoted to form more superoxide anion radical which makes N–TiO_2 active under low energy of visible light.

3.4. Mechanism of Ti–O–N formation

Based on the characterization of N–TiO_2, possible mechanism of Ti–O–N is proposed. The urea was decomposed under microwave treatment producing NH_3 and CO_2. Hence, the NH_3 can absorb the surface of TiO_2 and the nitridation process occurs [47]. As illustrated in Fig. 10, The Ti–O–N linkage can be formed by chemical binding of N atom from NH_3 with O atom in the TiO_2 where N–O and N–H bonds were confirmed by XPS and FTIR analysis. The Ti–O–N bond can be formed by N incorporation into pristine TiO_2

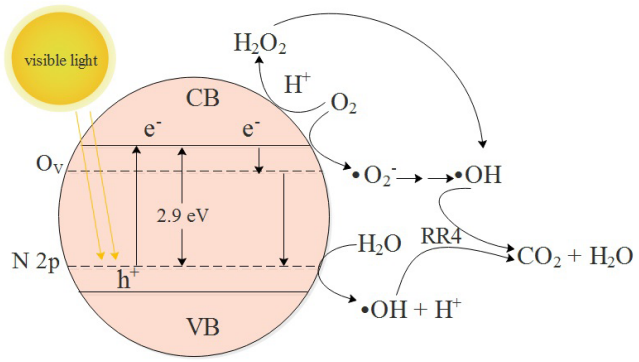

Fig. 9. Schematic diagram for the photodegradation of RR4 dye over interstitial N 2p N–TiO_2.

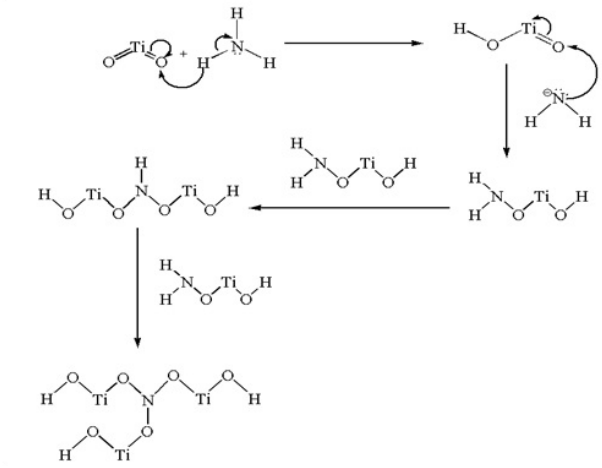

Fig. 10. Proposed mechanism of Ti–O–N in N–TiO_2.

by binding the O atoms with N atoms during the interaction between HO–Ti–O–NH_2 species. From this proposed mechanism, the incorporation of nitrogen into pristine TiO_2 can result as interstitial form.

4. Conclusion

A simple technique using physical preparation was successfully carried out for the preparation of visible light active interstitial N 2p N–TiO_2 by mixing urea and TiO_2 powder under microwave irradiation, which were used to decolourize RR4 dye under visible light. The interstitial N 2p was investigated based on the FTIR, XPS and XRD analyses. The FTIR result indicated that hyponitrite which assigned from N–H urea adsorbed is the characteristic of interstitial at 1,642 cm^{-1} and N–O bonding detected at 1,449 cm^{-1}. The XPS analysis identified that N is chemically bonded with titania crystal producing Ti–O–N linkage at the peaks 400.2 and 404.8 eV. XRD analysis shows that there is no TiN peak at $2\theta = 43°$ and no significant changes in N–TiO_2 compared with pristine TiO_2. N_2-adsorption surface area measurement shows N–TiO_2 produced low surface area compared with pristine TiO_2 due to solid-state sintering effect. Bandgap energy of N–TiO_2 was reduced to 2.9 eV as recorded by UV-Vis DRS spectrum. In addition, the presence of N makes N–TiO_2 active under

visible light irradiation. The preparation method of N–TiO_2 synthesized using physical method under microwave irradiation will promising a simple, cost-effective, low energy consumption and ecological toward becoming a great potential in application and development photocatalysis industry.

Acknowledgements

We would like to thank the Institute of Research Management and Innovation (IRMI) for providing generous financial support under REI grants: 600-IRMI/DANA 5/3/REI (1/2017) in conducting this study and Universiti Teknologi Mara (UiTM) for providing all the needed facilities.

References

[1] S. Sato, Photocatalytic activity of NOx-doped TiO_2 in the visible light region, Chem. Phys. Lett., 123 (1986) 126–128.
[2] R. Asahi, T. Morikawa, T. Ohwaki, K. Aoki, Y. Taga, Visible-light photocatalysis in nitrogen doped titanium oxides, Science, 293 (2001) 269–271.
[3] D.C. Valentin, G. Pacchioni, A. Selloni, Origin of the different photoactivity of N-doped anatase and rutile TiO_2, Phys. Rev. B, 70 (2004) 85116.
[4] D.C. Valentin, E. Finazzi, G. Pacchioni, A. Selloni, S. Livraghi, M.C. Paganini, E. Giamello, N-TiO_2: theory and experimental, Chem. Phys., 339 (2007) 44–56.
[5] A.V. Emeline, V.N. Kuznetsov, V.K. Rybchuk, N. Serpone, Visible-light-active titania photocatalysts: the case of N-TiO_2 properties and some fundamental issues, Int. J. Photoenergy, 2008 (2008) 1–19.
[6] X.P. Wang, T.T. Lim, Solvothermal synthesis of C-N codoped TiO_2 and photocatalytic evaluation for bisphenol a degradation using a visible-light irradiated led photoreactor, Appl. Catal., B, 100 (2010) 355–364.
[7] S. Bangkedphol, H.E. Keenan, C.M. Davidson, A.W. Sakultantimetha, Enhancement of tributyltin degradation under natural light by N-TiO_2 photocatalyst, J. Hazard. Mater., 184 (2010) 533–537.
[8] D. Chen, Z. Jiang, J. Geng, Q. Wang, D. Yang, Carbon and nitrogen co-doped TiO_2 with enhanced visible light photocatalytic activity, Ind. Eng. Chem. Res., 46 (2007) 2471–2746.
[9] F. Peng, L.F. Cai, H. Yu, H. Wang, J. Yang, Synthesis and characterization of substitutional and interstitial nitrogen-doped titanium dioxides with visible light photocatalytic activity, J. Solid State Chem., 181 (2008) 130–136.
[10] C.C. Hu, T.C. Hsu, L.H. Kao, One-step cohydrothermal synthesis of nitrogen-doped titanium oxide nanotubes with enhanced visible light photocatalytic activity, Int. J. Photoenergy, 2012 (2012) 1–9.
[11] J.A. Rengifo-Herrera, J. Kiwi, C. Pulgarin, N, S co-doped and N-doped Degussa P-25 powders with visible light response prepared by mechanical mixing of thiourea and urea. Reactivity towards *E. coli* inactivation and phenol oxidation, J. Photochem. Photobiol., A, 205 (2009) 109–115.
[12] I.C. Kang, Q. Zhang, S. Yin, T. Sato, F. Saito, Novel method for preparation of high visible active N-TiO_2 photocatalyst with its grinding in solvent, Appl. Catal., B, 84 (2008) 570–576.
[13] W.I. Nawawi, M.A. Nawi, Carbon coated nitrogen doped P25 for the photocatalytic removal of organic pollutants under solar and low energy visible light irradiations, J. Mol. Catal. A: Chem., 383–384 (2014) 83–93.
[14] C.H. Wu, C.Y. Kuo, C.J. Lin, P.K. Chiu, Preparation of N-TiO_2 using a microwave/sol-gel method and its photocatalytic activity for bisphenol a under visible-light and sunlight irradiation, Int. J. Photoenergy, 2013 (2013) 1–9.
[15] A.N. Kadam, R.S. Dhabbe, M.R. Kokate, Y.B. Gaikwad, K.M. Garadkar, Preparation of N-TiO_2 via microwave-assisted method and its photocatalytic activity for degradation of Malathion, Spectrochim. Acta, Part A, 133 (2014) 669–676.
[16] N.M. Mahmoodi, M. Arami, Immobilized titania nanophotocatalysis: degradation, modeling and toxicity reduction of agricultural pollutants, J. Alloys Compd., 506 (2010) 155–159.
[17] M. Janus, K. Bubacz, J. Zatorska, E. Kusiak-Nejman, A. Czyzewski, A.W. Morawski, Preliminary studies of photocatalytic activity of gypsum plasters containing TiO_2 co-modified with nitrogen and carbon, Pol. J. Chem. Technol., 17 (2015) 96–102.
[18] K.S. Virendra, P.B. Mandar, B.P. Aniruddha, Degradation of reactive red 120 dye using hydrodynamic cavitation, Chem. Eng. J., 178, (2011) 100–107.
[19] W.I. Nawawi, M.S. Azami, L.S. Ang, M.A.M. Ishak, K. Ismail, Modification and characterization of microwave assisted N doped TiO_2 – a photodegradation study under suspension and immobilized system, Water Qual. Res. J., 52 (2015) 51–63.
[20] Z. Zhang, X. Weng, K. Gong, J.A. Darr, Photocatalytic activity of nitrogen doped nano-titanias and titanium nitride towards methyl blue decolouration, NSTI Nanotech, 1 (2008) 680–683.
[21] Z. Wang, W. Cai, X. Hong, X. Zhao, F. Xu, C. Cai, Photocatalytic degradation of phenol in aqueous nitrogen-doped TiO_2 suspensions with various light sources, Appl. Catal., B, 57 (2005) 223–231.
[22] Z. Xie, Y. Zhang, X. Liu, W. Wang, P. Zhan, Z. Li, Z. Zhang, Visible light photoelectrochemical properties of N-TiO_2 nanorod arrays from TiN, J. Nanomater., 2013 (2013) 1–8.
[23] H.R. An, H.L. An, W.B. Kim, H.J. Ahn, Nitrogen-TiO_2 nanoparticle-carbon nanofiber composites as a counter electrode for Pt-Free dye-sensitized solar cells, ECS Solid State Lett., 3 (2014) 33–36.
[24] K. Masaaki, F. Keisho, M. Masaya, U. Michio, A. Masakazu, Preparation of nitrogen-substituted TiO_2 thin film photocatalysts by the radio frequency magnetron sputtering deposition method and their photocatalytic reactivity under visible light irradiation, 110 (2006) 25266–25272.
[25] F. Hiroki, G.L. Carlos, W.Z. Frank, Controlling mechanical properties of porous mullite/alumina mixtures via precursor-derived alumina, J. Am. Ceram. Soc., 2 (2005) 367–375.
[26] X.T. Zhou, H.B. Ji, X.-J, Huang, Photocatalytic degradation of methyl orange over metalloporphyrins supported on TiO_2 degussa P25, Molecules, 17 (2012) 1149–1158.
[27] Y. Hu, H. Liu, X. Kong, X. Guo, Effect of calcination on the visible light photocatalytic activity of N-TiO_2 prepared by the sol-gel method, J. Nanosci. Nanotechnol., 13 (2013) 1–6.
[28] D. Huang, S. Liao, S. Quan, L. Liu, Z. He, J. Wan, W. Zhou, Synthesis and characterization of visible light responsive N–TiO_2 mixed crystal by a modified hydrothermal process, J. Non-Cryst. Solids, 354 (2008) 3965–3972.
[29] M. Sathish, B. Viswanathan, R.P. Viswanath, Characterization and photocatalytic activity of N-TiO_2 prepared by thermal decomposition of Ti–melamine complex, Appl. Catal., B, 74 (2007) 307–312.
[30] H.M. Yates, M.G. Nolan, D.W. Sheel, M.E. Pemble, The role of nitrogen doping on the development of visible light-induced photocatalytic activity in thin TiO_2 films grown on glass by chemical vapour deposition, J. Photochem. Photobiol., A, 179 (2006) 213–223.
[31] Y.K. Chao, H.Y. Ya, Exploring the photodegradation of bisphenol A in a sunlight/immobilized N-TiO_2 system, Pol. J. Environ. Stud., 23 (2014) 379–384.
[32] Y.T. Lin, C.H. Weng, H.J. Hsu, Y.H. Lin, C.C. Shiesh, The synergistic effect of nitrogen dopant and calcination temperature on the visible-light-induced photoactivity of N-TiO_2, Int. J. Photoenergy, 2013 (2013) 1–13.
[33] L. Zhu, J. Xie, X. Cui, J. Shen, X. Yang, Z. Zhang, Photoelectrochemical and optical properties of N-TiO_2 thin films prepared by oxidation of sputtered TiN_x films, Vacuum, 84 (2010) 797–802.
[34] K.S. Rane, R. Mhalsiker, S. Yin, T. Sato, K. Cho, E. Dunbar, P. Biswas, Visible light-sensitive yellow $TiO_{2-x}N_x$ and Fe-N co-doped. $Ti_{1-y}Fe_yO_{2-x}N_x$ anatase photocatalysts, J. Solid State Chem., 179 (2006) 3033–3044.

[35] V. Etacheri, M. Seery, J. Hinder, S. Pillai, Nanostructured $Ti_{1-x}S_xO_{2-y}N_y$ heterojunctions for efficient visible-light-induced photocatalysis, Inorg. Chem., 51 (2012) 7164–7173.
[36] M. Sathish, B. Viswanathan, R.P. Viswanath, C.S. Gopinath, Synthesis, characterization, electronic structure, and photocatalytic activity of nitrogen-TiO_2 nanocatalyst, Chem. Mater., 17 (2005) 6349–6353.
[37] G. Yang, Z. Jiang, H. Shi, T. Xiao, Z. Yan, Preparation of highly visible-light active N-TiO_2 photocatalyst, J. Mater. Chem., 20 (2010) 5301–5309.
[38] Y.G. Zhang, L.L. Ma, J.L. Li, Y. Yu, In situ Fenton reagent generated from TiO_2/Cu_2O composite film: a new way to utilize TiO_2 under visible light irradiation, Environ. Sci. Technol., 41 (2007) 6264–6269.
[39] Y. Wang, M. Jing, M. Zhang, J. Yang, Facile synthesis and photocatalytic activity of platinum decorated $TiO_{2-x}N_x$: perspective to oxygen vacancies and chemical state of dopants, Catal. Commun., 20 (2012) 46–50.
[40] J. Tauc, A. Menth, State in the band gap, J. Non-Cryst. Solids, 11 (1972) 569–585.
[41] F. Peng, L. Cai, L. Huang, H. Yu, H. Wang, Preparation of nitrogen-doped titanium dioxide with visible light photocatalytic activity using a facile hydrothermal method, J. Phys. Chem. Solids, 69 (2008) 1657–1664.
[42] W.I. Nawawi, M.A. Nawi, Electron scavenger of thin layer Carbon coated and Nitrogen doped P25 with enhanced photocatalytic activity under visible light fluorescent lamp, J. Mol. Catal. A: Chem., 374–375 (2013) 39–45.
[43] W. Kim, T. Tachikawa, H. Kim, N. Lakshminarasimhan, P. Murugan, H. Park, T. Majima, W. Choi, Visible light photocatalytic activities of nitrogen and platinum-doped TiO_2: synergistic effects of co-dopants, Appl. Catal., B, 147 (2014) 642– 650.
[44] H. Wang, X. Gao, G. Duan, X. Yang, X. Liu, Facile preparation of anatase-brookite-rutile mixed-phase N-TiO_2 with high visible-light photocatalytic activity, J. Environ. Chem. Eng., 3 (2015) 603–608.
[45] C.W. Dunnilla, I.P. Parkin, Nitrogen-doped TiO_2 thin films: photocatalytic applications for healthcare environments, Dalton Trans., 40 (2011) 1635–1640.
[46] Z. Li, Y. Zhu, F. Pang, H. Liu, X. Gao, W. Ou, J. Liu, X. Wang, X. Cheng, Y. Zhang, Synthesis of N doped and N, S co-doped 3D TiO_2 hollow spheres with enhanced photocatalytic efficiency under nature sunlight, Ceram. Int., 41 (2015) 10063–10069.
[47] K. Kalantari, M. Kalbasi, M. Sohrabi, S.J. Royaee, Synthesis and characterization of N-doped TiO_2 nanoparticles and their application in photocatalytic oxidation of dibenzothiophene under visible light, Ceram. Int., 42 (2016) 2016.